Electronic Structure of Plastocyanin: Excited State Spectral Features

Andrew A. Gewirth and Edward I. Solomon*

Contribution from the Department of Chemistry, Stanford University, Stanford, California 94305. *Received August 10, 1987*

Abstract: Low-temperature optical absorption and MCD and CD spectra in conjunction with self-consistent field-Xα-scattered wave (SCF-Xα-SW) calculations are presented for the blue copper active site in plastocyanin. These spectral studies allow quantitative determination of the number, intensities, and MCD parameters of the blue copper absorption bands. Transitions strong in absorption are found to be generally weak in low-temperature MCD (LTMCD), while the opposite is true for weak absorption bands. Xα-SW calculations performed with sphere radii adjusted so that the ground state reproduces the experimental g values clearly separate ligand field and charge-transfer band energies. The results of these calculations are used to further calculate oscillator strengths and MCD parameters. This protocol is tested through application to both D_{2d} and D_{4h} symmetry tetrachlorocuprates where comparison with definitive experimental assignments is possible. The four lowest energy bands in the blue copper spectrum which are weak in absorption but strong in LTMCD are found to be ligand field transitions with the ordering $d_{x^2-y^2} \leftarrow d_{z^2} < \leftarrow d_{xy} < \leftarrow d_{xy+yz} < \leftarrow d_{xz-yz}$ in the C_s-perturbed, elongated C_{3v} blue copper site. The intense blue band at 600 nm is found to be a cysteine S $p\pi \rightarrow d_{x^2-y^2}$ transition which gets its intensity from the extremely good overlap between the ground- and excited-state wave functions. The blue band has the correct symmetry to allow for configuration interaction with the d_{xz+yz} orbital and thus gives intensity to this lower energy 780-nm transition. A transition from the pseudo-σ orbital of the thiolate is predicted to have little intensity due to poor overlap with the ground-state $d_{x^2-y^2}$ orbital and is responsible for the weak band on the high-energy side of the blue band (at 535 nm). Finally histidine π_1 and thioether a_1 transitions are assigned to very weak bands in the region of 425-465 nm. This assignment provides further insight into the bonding at the plastocyanin site. The large splitting between the $d_{x^2-y^2}$ and d_{xy} orbitals reflects the presence of a quite strong cysteine S$p\pi$ interaction with the copper which is responsible for the orientation of the $d_{x^2-y^2}$ ground-state orbital. The low energy of the d_{z^2} orbital indicates a reasonable interaction between the copper and the thioether S at a 2.9 Å bond length. Finally, it is determined that the thiolate-copper(II) bond makes a dominant contribution to the electronic structure of the blue copper active site which can be strongly influenced by the orientation of this residue by the protein backbone. Thus, changes in spectral features correlated with changes in the thiolate bond in different blue copper proteins are described.

1. Introduction

Blue copper proteins have high redox potentials and facile rates of electron transfer relative to normal copper complexes. The development of a detailed understanding of the unique spectroscopic features of the blue copper site has been a major goal of many experimental and theoretical studies.[1-11] The most striking spectroscopic feature associated with the blue copper center is its intense blue color resulting from absorption at energies around 17000 cm^{-1}. This absorption is two orders of magnitude greater than that found with normal tetragonal complexes ($\epsilon \cong 5000$ M^{-1} cm^{-1} versus <100 M^{-1} cm^{-1}) in the same energy region. An understanding of the origin of this intense absorption band is important both from a spectroscopic point of view and in order to provide further insight into the electronic structure of the blue copper active site and its contribution to reactivity.

The first efforts directed at understanding this intense blue color ascribed it to a ligand field transition gaining intensity due to $4p_z$ mixing into the Cu center.[2] This mixing would derive from the low symmetry of the copper site. $4p_z$ mixing was also invoked to explain the small hyperfine coupling also associated with these centers. A major advance in understanding the absorption spectrum of the blue copper proteins was the observation[12] of at least three transitions in the energy region between 12000 and 5000 cm^{-1}, a feature which required the site to have approximately tetrahedral geometry. In addition, as peaks associated with all the d-d transitions were observed at energies below the 600-nm band, the dominant feature of the blue copper absorption spectrum had to be a ligand-to-metal charge-transfer (CT) transition. Since other chemical and spectral data indicated that a thiolate sulfur of a cysteine residue was a ligand associated with the site, this appeared to be a likely assignment for the low-energy CT transition. The subsequent appearance of a high resolution crystal structure of the blue copper site in plastocyanin[13] confirmed the approximately tetrahedral nature of the site and the thiolate sulfur coordination. In addition, the crystal structure identified the remaining three ligands as two nitrogens from imidazoles of histidine residues and a sulfur of the thioether of a methionine residue with a long bond of 2.9 Å.

Single-crystal EPR spectroscopy on plastocyanin[6] in conjunction with a crystal field calculation indicated that the blue copper site was best described as having elongated C_{3v} effective symmetry with rhombic distortions, the long axis being directed approximately along the Cu-S(met) bond. Further, polarized optical studies[6] indicated that the intense bands in the absorption spectrum were polarized in a manner consistent with their being related to charge transfer from the cysteine sulfur.

(1) Fee, J. A. *Struct. Bonding (Berlin)* **1975**, *23*, 1-60.
(2) Brill, A. S.; Bryce, G. F. *J. Chem. Phys.* **1968**, *48*, 4398.
(3) Blumberg, W. E.; Peisach, J. *Biochem. Biophys. Acta* **1966**, *126*, 269.
(4) Gray, H. B.; Solomon, E. I. In *Copper Proteins*; Spiro, T. G., Ed.; Wiley: New York, 1981; pp 1-39.
(5) Solomon, E. I.; Penfield, K. W.; Wilcox, D. E. *Struct. Bonding (Berlin)* **1983**, *53*, 1-57.
(6) Penfield, K. W.; Gay, R. R.; Himmelwright, R. S.; Eickman, N. C.; Norris, V. A.; Freeman, H. C.; Solomon, E. I. *J. Am. Chem. Soc.* **1981**, *103*, 4382.
(7) Penfield, K. W.; Gewirth, A. A.; Solomon, E. I. *J. Am. Chem. Soc.* **1985**, *107*, 4519.
(8) Dorfman, R.; Bereman, X.; Whangbo, M. In *Copper Coordination Chemistry: Biochemical and Inorganic Perspectives*; Karlin, K., Zubieta, J., Eds.; Adenine Press: Guilderland, NY, 1982.
(9) Blair, D. F.; Campbell, G. W.; Schoonover, J. R.; Chan, S. I.; Gray, H. B.; Malmstrom, B. G.; Pecht, I.; Swanson, B. I.; Woodruff, W. H.; Cho, W. K.; English, A. M.; Fry, H. A.; Lum, V.; Norton, K. A. *J. Am. Chem. Soc.* **1985**, *107*, 5755.
(10) Roberts, J. E.; Cline, J. F.; Lum, V.; Freeman, H. C.; Gray, H. B.; Reisach, J.; Reinhammer, B.; Hoffman, B. *J. Am. Chem. Soc.* **1984**, *106*, 5324.
(11) Scott, R. A.; Hahn, J. E.; Boniach, S.; Freeman, H. C.; Hodgson, K. O. *J. Am. Chem. Soc.* **1985**, *107*, 5755.
(12) (a) Solomon, E. I.; Hare, J. W.; Gray, H. B. *Proc. Natl. Acad. Sci. U.S.A.* **1976**, *73*, 1389. (b) Solomon, E. I.; Hare, J. W.; Dooley, D. M.; Dawson, J. H.; Stephens, P. J.; Gray, H. B. *J. Am. Chem. Soc.* **1980**, *102*, 168.
(13) Guss, J. M.; Freeman, H. C. *J. Mol. Biol.* **1983**, *169*, 521.

0002-7863/88/1510-3811$01.50/0

Finally, experimentally calibrated self-consistent field-Xα-scattered wave (SCF-Xα-SW) calculations[7] indicated that the ground state in the blue copper center was characterized by substantial anisotropic delocalization over the Cu $d_{x^2-y^2}$ and cysteine Spπ orbital. This delocalization was used to explain the hitherto anomalous ground-state EPR parameters (the small parallel hyperfine splitting $A_{\parallel} < 70 \times 10^{-4}$ cm^{-1}) associated with blue copper sites.

The insight achieved for the ground state in plastocyanin is now extended to excited states in order to describe in detail the bonding interactions which make up the site. The approach taken here is to generate a detailed experimental assignment of the absorption spectrum of plastocyanin by using the different selection rules provided by absorption, CD, and low-temperature MCD techniques. Further, the adjusted sphere Xα protocol developed previously[14,15] is used to calculate transition energies, oscillator strengths, and MCD parameters in order to compare with experiment. These Xα calculations in conjunction with experiment provide a detailed description of the interactions between the copper and the ligands in the blue site and their contributions to the electronic structure. These studies provide insight into the high reactivity of the blue copper site and its variation over different proteins.

2. Experimental Section

Plastocyanin was isolated from spinach chloroplasts by standard methods.[16] The A_{597}/A_{278} ratio was one in the samples used for MCD.

MCD spectra of plastocyanin glasses containing 50% (v/v) glycerol in 0.1 M PO_4^{5-} pH 6.0 were obtained at temperatures between 1.9 and 290 K and fields up to 6 T by using a JASCO J-500C CD spectrometer equipped with an Oxford Instruments SM4 superconducting magnet. Depolarization was checked by placing a solution of (+) nickel tartarate before and after the sample and monitoring the change in its CD. In all cases the depolarization was less than 1%.

Standard versions of spin unrestricted SCF-Xα-SW calculations were performed on Vax computers with computation times ranging between 15 and 55 min per iteration and with between 50 and 100 iterations required for convergence. In order to allow rapid variation of sphere radii and inclusion of high azimuthal quantum numbers into the calculation (vida infra), the C_s(met) approximation to the plastocyanin site[7] was used in the calculations. This approximation having molecular formula Cu-$(S(CH_3)_2)(SCH_3)(NH_3)_2^+$ replaces the imidazoles of histidine (His 87 and His 37) with ammines, the cysteine thiolate (Cys 84) with methyl thiolate, and the methionine thioether (Met 92) with dimethyl thioether. The Cu–S(cys) bond length was 2.13 Å, and the Cu–S(cys)–C(cys) bond angle was 109°, while the Cu–S(met) bond length was 2.90 Å, and the angle between the plane formed by the thioether and the Cu–S(met) bond was 50°. In addition, the Cu–N bond lengths are averaged to 2.07 Å (plastocyanin crystal structure:[13] Cu–N (His 87) = 2.10 Å; Cu–N (His 37) = 2.04 Å), and a mirror plane imposed so that S(met), Cu, S(cys), and C(cys) were all coplanar (plastocyanin crystal structure: dihedral angle between planes formed by S(met)–Cu–S(cys) and Cu–S(cys)–C(cys) = 4°). We have previously shown[7] that this approximation yields results very similar to those obtained with the plastocyanin crystal structure coordinates (i.e., the C_1 calculation in ref 7). Additional geometries are described in the text.

Sphere radii were chosen by fitting the calculation to the experimental ground-state g values and at the same time matching the calculated potentials at the sphere boundaries. This sphere radii adjustment procedure has been found to give ground-state metal character in agreement with that determined by using independent methods[14,17] and generally gives more metal character in the ground state than do calculations performed by using Norman's[18] criteria for sphere radii.[15] For the C_s-(met) calculation the sphere radii were Cu, 2.95 bohr; S(cys), 2.50 bohr; S(met), 2.2 bohr; N, 1.90 bohr; all carbons, 1.80 bohr; and all H, 1.17 bohr. In these calculations, the copper and sulfur radii were close to those determined previously[14] for copper and chlorine in the chlorocuprates. The α values were those determined by Schwarz,[19] while a tangental

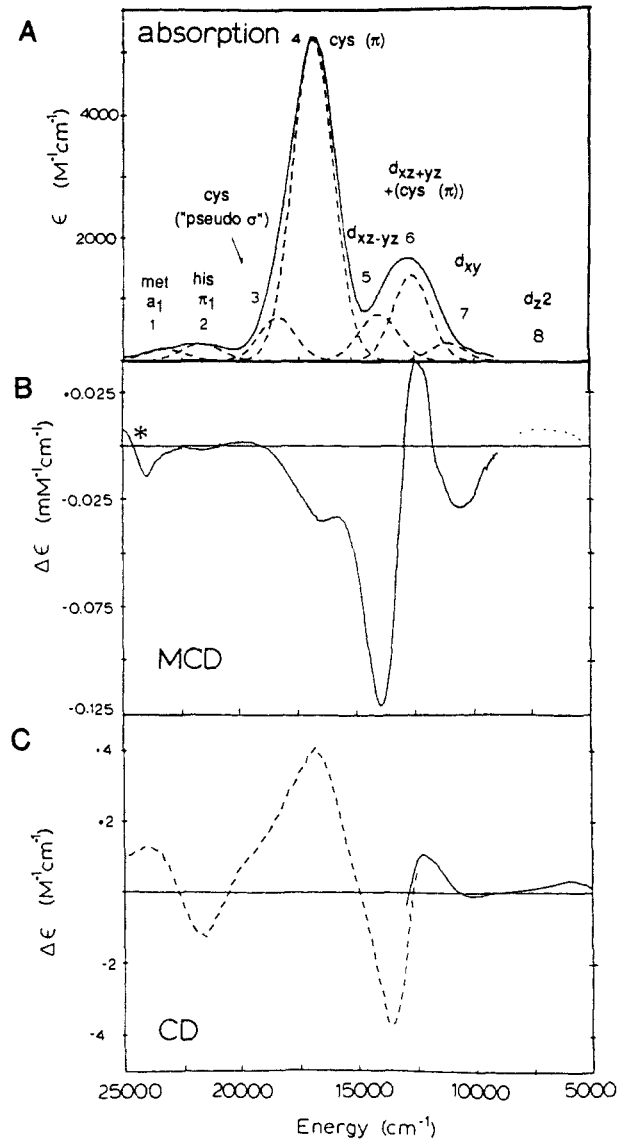

Figure 1. (A) Absorption spectrum (25 K) of a plastocyanin film (from ref 4). Gaussian resolution of bands, numbering scheme, and assignments are indicated in the text. Band 0, at 32 500 cm^{-1} is not shown. (B) MCD spectrum (4.5 K, 4 T) of spinach plastocyanin glass containing 0.05 M phosphate pH 6.0 and 50% (v/v) glycerol. Sample concentration was 1.20 mM. Dashed line indicates lowest energy band placed by analogy with azurin[20] and stellacyanin[21] data. (C) Room (solid line) and 4.5 K (dashed line) CD. Room temperature data from ref 12.

Watson sphere was used in all calculations of charged species. Optical transition energies were determined by using the Slater transition state.

3. Results and Analysis

3.1. Absorption, CD, and MCD Spectroscopy. Low-temperature absorption[12] and MCD and CD spectra for plastocyanin in the energy region from 5000 to 25 000 cm^{-1} are presented in Figure 1. MCD has already been obtained for azurin[20] and stellacyanin;[21] however, single-crystal optical spectra are not available for either of these blue proteins, and it is thus necessary to extend MCD studies to plastocyanin in order to correlate it with the single-crystal data. Overtones from water obscure the absorption spectrum in the 5000–9000-cm^{-1} range, while our instrument limitations precluded taking MCD data at energies less than 9000 cm^{-1}.[22] However, plastocyanin shares a positive

(14) Gewirth, A. A.; Cohen, S. L.; Schugar, H. J.; Solomon, E. I. *Inorg. Chem.* **1987**, *26*, 1133.
(15) Bencini, A.; Gatteschi, B. *J. Am. Chem. Soc.* **1983**, *105*, 5535.
(16) Ellefson, W. L.; Ulrich, E. A.; Krogmann, D. W. In *Methods in Enzymology, Vol. 69*; San Pietro, A., Ed.; McGraw-Hill: New York, 1980; pp 223–28.
(17) Solomon, E. I.; Gewirth, A. A.; Cohen, S. L. In *Understanding Molecular Properties*; Avery, J., Dahl, J. P., Eds.; Reidel: Dortrecht, 1987.
(18) Norman, J. G. *Mol. Phys.* **1976**, *31*, 1191.
(19) Schwartz, K. *Phys. Rev. B* **1972**, *5*, 2466.
(20) Barrett, C. P.; Peterson, J.; Greenwood, C.; Thomson, A. J. *J. Am. Chem. Soc.* **1986**, *108*, 3170.
(21) Peterson, C. G.; Gewirth, A. A.; Penfield, K. W.; Thomson, A. J.; Solomon, E. I., to be published.
(22) Spira-Solomon, D. J.; Allendorf, M. D.; Solomon, E. I. *J. Am. Chem. Soc.* **1986**, *108*, 5318.

Table I. Experimental Spectroscopic Parameters for Spinach Plastocyanin

band	energy (cm^{-1})	ϵ (M^{-1} cm^{-1})	oscillstr strength	$\Delta\epsilon$ at 4 T, 5K (mM^{-1} cm^{-1})	C/D
8	5000				(+)
7	10800	250	0.0031	−0.0287	−0.171
6	12800	1425	0.0114	+0.0712	+0.076
5	13950	500	0.0043	−0.1410	−0.409
4	16700	5160	0.0496	−0.0324	−0.009
3	18700	600	0.0048	+0.0041	+0.011
2	21390	288	0.0035	−0.0016	−0.009
1	23440				(−)
0	32500				(−)

CD feature in the energy region around 5000 cm^{-1} with the blue copper proteins stellacyanin and azurin.[12] As both of these proteins have a positive MCD feature[12] (which is also present in the LTMCD spectrum[21]) corresponding to the CD feature at this energy, it is reasonable to place a positive MCD feature around 5000 cm^{-1} in plastocyanin with approximately the same amplitude as in azurin. This feature is represented by a dotted line in Figure 1B. The derivative-shaped feature (denoted by a star in Figure 1B) centered around 24400 cm^{-1} in the MCD spectrum of plastocyanin is attributed to limited (<1%) heme contamination of the sample. MCD bands at energies less than this feature gave saturation–magnetization curves[23] with g values of 2.2 and show temperature dependence consistent with their being entirely C terms,[24] characteristic of mononuclear copper(II) at these temperatures. However, bands to higher energy from the heme feature exhibit saturation–magnetization curves with substantially higher g values ($g_{\parallel} \sim 2.8$). Azurin also shows heme contamination in this region.[20] Nonetheless, differing amounts of the heme impurity in different samples allows identification of two negative MCD features attributable to Cu at 23400 and 32500 cm^{-1}. Finally, at energies between 33000 and 40000 cm^{-1}, the MCD spectrum was temperature-independent indicating no contribution from copper in this region. The combination of low-temperature MCD and absorption spectra allows unambiguous determination of the number, energy, and intensity of bands in plastocyanin.

Figure 1 also gives a Gaussian resolution of the bands in the plastocyanin absorption spectrum from a simultaneous fit of the low-temperature absorption and low-temperature MCD data, while Table I gives energies, absorption intensities, and MCD parameters for the bands.[25] Here, we have preserved the numbering scheme used previously.[6] The linear region of the saturation–magnetization curve can be used to find the MCD signal which is proportional to $1/T$ yielding the MCD C-term. The ratio of this MCD C-term intensity (C) to oscillator strength (D) is given in the last column of Table I. Significantly, bands 7 and 5, which are among the weakest in absorption, have the highest C/D ratios. Alternatively, the two strongest bands in absorption, bands 6 and 4, give rise to relatively small C/D ratios.

3.2. Results of Xα Calculations. The Xα-SW calculated ground-state energies and one-electron orbitals for the C_s(met) approximation to the plastocyanin site are presented in Table II. These results are similar to those obtained previously[7] by using the Norman criteria for the sphere radii. In agreement with our previous use of a single adjustable parameter[7] to correct for the overestimation of delocalization arising from use of the Norman criteria for the sphere radii, these adjusted sphere results also indicate 42 ± 3% metal character in the ground state. However, the adjusted sphere radii calculation presented here more clearly energetically separates the antibonding d levels and bonding ligand orbitals. A similar effect has been found for the chlorocuprates.[15,17] Finally, the Xα calculations indicate that the cystine sulfur in the

Table II. Results of SCF-Xα-SW Calculation for the Highest Occupied Valence Levels of the C_s(met) Site Giving Ground-State Orbital Energies and Charge Distribution[a]

level	energy (eV)	character
12a″	−4.931	42% Cu [$d_{x^2-y^2}$] (ab) 36% S_{cys} p_π + 4% N
18a′	−5.131	20% Cu [0.8 d_{z^2} + 0.5 d_{xy}] (ab) 49% S_{met} p_y
17a′	−5.818	73% Cu [0.9 d_{xy}] (ab) 9% $S_{cys}\sigma$
11a″	−6.295	75% Cu [0.9 d_{xz+yz}] (b) 14% S_{cys} p_π
16a′	−6.260	84% Cu [0.8 d_{xx-yz} + 0.4 d_{z^2}]
15a′	−6.451	89% Cu [0.8 d_{z^2} + 0.5 d_{xz-yz}] (b) 5% S_{met} p_y
10a″	−6.700	69% Cu [0.8 d_{xy+yz} + 0.6 $d_{x^2-y^2}$] (b) 21% S_{cys} p_π
14a′	−7.879	31% Cu [0.9 d_{xy}] (b) 55% S_{cys} pseudo-σ
13a′	−7.954	10% Cu [0.85 d_{z^2}] (b) 46% S_{met} p_z
12a′	−10.513	18% Cu [0.7 d_{xy}] (b) 47% $S_{cys}\sigma$

[a] (ab) Denotes antibonding interaction; (b) denotes bonding interaction.

Table III. Calculated Transition Energies, Oscillator Strengths, and C/D Ratios for the C_s(met) Site

level	transition energy (cm^{-1})	oscillstor strength ΔV	oscillstor strength lig. ovlp.	C/D
18a′	4527	1.2×10^{0}	5.5×10^{-6}	+0.996
17a′	8691	1.5×10^{-1}	4.6×10^{-5}	−0.687
11a″	11942	5.2×10^{-2}	4.6×10^{-2}	+0.012
16a′	15064	2.3×10^{-3}	2.2×10^{-5}	−0.145
15a′	15895	1.5×10^{-4}	1.3×10^{-5}	+0.019
10a″	16940	8.3×10^{-2}	7.8×10^{-2}	+0.015
14a′	25313	1.1×10^{-3}	1.0×10^{-4}	−0.548
13a′	36700	2.1×10^{-6}	3.5×10^{-5}	−0.487
12a′	47685	4.3×10^{-4}		

occupied levels is almost entirely p orbital in character; no level contains more than 2% sulfur d contribution.

Table III gives the calculated transition state energies for the C_s(met) site. Again, ligand field transitions (from orbitals with primarily antibonding character) are lower in energy than those arising from charge-transfer transitions (from bonding levels).

3.3. Calculation of Oscillator Strengths and MCD C/D Ratios. A. Oscillator Strengths. In order to gain insight into intensity mechanisms operative in the blue copper active site and in particular the source of the high intensity for bands 4 and 6, we have used two methods of calculating oscillator strengths from the Xα wave function. First, within the Xα formalism, Noodleman[26] has derived a density matrix formulation for optical absorption by using the transition state concept. Here, the acceleration form of the oscillator strength is used on transition state orbitals. The oscillator strength is given by

$$f_{1\to 2} = \frac{2\hbar^2}{3m(\Delta E)^3}\langle \mu_1^T|\nabla V|\mu_2^T\rangle \qquad (1)$$

where $\mu_{1,2}^T$ are the initial and final one-electron molecular orbitals in the transition state created by promoting one-half electron from orbital 1 to orbital 2, and ΔE is the transition energy. In the Xα-SW calculation, eq 1 reduces to a sum of atomic overlaps adjusted by the transition state. These oscillator strength calculations converge slowly with increasing aximuthal quantum number l, and it is important to use relatively large l values on both the metal and ligand centers.

The second method of oscillator strength calculation uses the approximation given by van der Avroid and Ros[27] which was first applied to Xα wave functions by Desjardins et al.[28] Here, overlaps involving metal-centered terms are neglected, and the oscillator strength reduces to a sum of overlaps between the ligand orbital contribution (ϕ_L) in the ground and excited molecular orbitals. Thus, the oscillator strength is given by

$$f = 1.085 \times 10^{11}(\Delta E)|D|^2 \qquad (2)$$

(23) Johnson, M. K.; Thomson, A. J. *Biochem. J.* **1980**, *191*, 411.
(24) Stephens, P. J. *Adv. Chem. Phys.* **1976**, *35*, 197.
(25) The LTMCD data enables more accurate determination of the spectroscopic parameters for plastocyanin than that given previously in ref 11. While the number and energies of the bands is the same both here and in ref 11, the Gaussian analysis here gives relatively more intensity to band 6 and relatively less to bands 3 and 5.

(26) Noodleman, L. *J. Chem. Phys.* **1976**, *64*, 2343.
(27) van der Avoird, A.; Ros, P. *Theor. Chim. Acta* **1966**, *4*, 13.
(28) Desjardins, S. R.; Penfield, K. W.; Cohen, S. L.; Musselman, R. L.; Solomon, E. I. *J. Am. Chem. Soc.* **1983**, *105*, 4590.

where

$$D = \langle \phi_{L,1}|r|\phi_{L,2}\rangle = \sum_a C_{a,1}C_{a,2}r_a \quad (3)$$

Here, C_1 and C_2 are coefficients, r is the position vector of ligand a, and ΔE is again the transition energy. This method has been used[28] to calculate oscillator strengths in D_{4h} and D_{2d} chlorocuprates with Xα sphere radii determined from the Norman criteria. The results of both oscillator strength calculations for the C_s(met) approximation to the plastocyanin site are included in Table III. It should be noted that the ligand overlap approach indicates that the 11a″ and 10a″ transitions have an order of magnitude more intensity than all the other transitions. The density matrix approach also indicates that these two transitions are strong but additionally predicts highest intensity in the two lowest energy transitions 18a′ and 17a′ which is inconsistent with experiment.

B. MCD *C* terms. The Xα charge distribution can also be used to calculate MCD C terms. For a randomly oriented molecule, parameters are related to the electronic structure of the complex via[29]

$$C_0 = -\frac{i}{3|A|}\sum_{\alpha\alpha'\lambda} \langle A\alpha'|(\mathbf{L} + 2\mathbf{S})|A\alpha\rangle\cdot(\langle A\alpha|\mathbf{m}|J\lambda\rangle \times \langle J\lambda|\mathbf{m}|A\alpha'\rangle) \quad (4)$$

Here, A and J represent the spin-orbit corrected ground and excited states, respectively, $\mathbf{L} + 2\mathbf{S}$ is the Zeeman operator, $\mathbf{m}$ is the transition moment operator, $|A|$ denotes the degeneracy of A (equal to 2 for copper), and the sum is over components of the Kramers doublet in the ground (α,α') and excited (λ) states. Brill[30] has developed perturbation expressions to evaluate eq 4 assuming D_2 symmetry and a hybrid atomic orbital model explicitly invoking p_z mixing into the ground state. Experimentally however only $4p_{x,y}$ mixing is found in the ground state of plastocyanin.[31,32]

Our approach to evaluating eq 4 parallels the g value calculation we used previously.[7] The Xα partitioned charge distribution is orthogonalized by using either the Gram–Schmidt or Löwdin (symmetric) techniques.[33] Spin-orbit coupling is added in a complete calculation, and the appropriate Zeeman and oscillator strength matrix elements (using the ligand overlap method described above) are evaluated. It should be noted that as long as the oscillator strength calculation gives the correct polarization for the transition under consideration, the calculated C/D ratio will be independent of the calculated magnitude of the oscillator strength. The results for plastocyanin are also presented in Table III. It is important to note that the 18a′, 17a′, and 16a′ levels are calculated to have large values of C/D while the 10a″ and 11a″ levels which are strongest in absorption are calculated to have relatively low MCD intensities.

3.4. Application to Model Complexes. Before analysis of the results for plastocyanin, it is important to test the validity of these methods of calculating transition energies, oscillator strengths, and MCD C/D ratios with the adjusted sphere Xα-SW calculation by applying these methods to the symmetry-allowed ligand field and CT transitions in the chlorocuprates where comparison with definitive experimental assignments[28] is possible. Calculations were performed for both the D_{2d} and D_{4h} chlorocuprate geometries by using the adjusted sphere radii determined previously.[14] Table IV presents experimental and calculated transition energies and oscillator strengths for the ligand-field and charge-transfer transitions of the D_{4h} and D_{2d} geometries of $CuCl_4^{2-}$. The ligand-field and charge-transfer transition energies for D_{4h} $CuCl_4^{2-}$ are quite good with respect to experiment,[28,34] while for D_{2d} $CuCl_4^{2-}$, the CT transitions are calculated somewhat higher in energy than is experimentally observed.[35] It is also apparent that both oscillator strength calculations perform quite well with respect to experiment[28,36] in the CT region; however, the acceleration form calculation does overestimate the intensity of the $4a_1 \rightarrow 5b_2$ ($d_{z^2} \rightarrow d_{x^2-y^2}$) transition in D_{2d} $CuCl_4^{2-}$ by two orders of magnitude. If the calculation is repeated with maximum l values of 8 and 5 on the copper and chlorine centers, respectively (as opposed to 5 and 2 originally), the calculated intensity of this transition decreases by a factor of two but is still far away from the experimental value. Thus, the results of the ∇V method should be viewed with caution when calculating intensities for ligand-field transitions.

Table IV. Experimental and Calculated Transition Energies and Oscillator Strengths for D_{4h} and D_{2d} $CuCl_4^{2-}$ in the Ligand Field (LF) and Charge Transfer (CT) Spectral Regions

		energy (cm^{-1})		oscillr strength		
salt	transition	calcd	exp	∇V	lig. ovlp	exp
D_{4h}						
LF[a]	$2b_{2g} \rightarrow 3b_{1g}$	12 308	12 500			*e*
	$3e_g \rightarrow 3b_{1g}$	12 247	14 250			
	$3a_{1g} \rightarrow 3b_{1g}$	16 038	17 000			
CT[b]	$1a_{2g} \rightarrow 3b_{1g}$	22 880	23 700			
	$1b_{2u} \rightarrow 3b_{1g}$	21 600		0.001	0.000	
	$4e_u \rightarrow 3b_{1g}$	27 460	26 400	0.032	0.036	0.055
	$3e_u \rightarrow 3b_{1g}$	38 430	37 400	0.192	0.205	0.405
D_{2d}						
LF[c]	$6e \rightarrow 5b_2$	4 263	4 500	0.009	0.005	0.003
	$2b_1 \rightarrow 5b_2$	6 599	7 200			
	$4a_1 \rightarrow 5b_2$	7 158	9 200	0.126	0.007	0.003
CT[b,d]	$3a_2 \rightarrow 5b_2$	27 920	22 700	0.012	0.004	
	$5e \rightarrow 5b_2$	28 860	24 730	0.032	0.022	0.050
	$4e \rightarrow 5b_2$	33 210	28 880	0.004	0.009	0.008
	$3e \rightarrow 5b_2$	39 780	33 480	0.096	0.081	0.091
	$2a_1 \rightarrow 5b_2$	46 140	43 000	0.075	0.053	0.030

[a] Reference 34. [b] Reference 28. [c] Reference 35. [d] Reference 36. [e] Vibronic intensity mechanism not considered here.

With respect to MCD in D_{2d} $CuCl_4^{2-}$, Briat[36] has identified three different types of transitions from the ground-state $d_{x^2-y^2}$ orbital. In all these types of transitions, spin-orbit coupling is required for nonzero C term intensity. This can be shown by considering the expression in eq 4. If spin-orbit coupling is not included in the wave function $\langle A\alpha|$, then C will sum to zero since $\langle A\alpha|\mathbf{L} + 2\mathbf{S}|A\alpha\rangle = -\langle A\beta|\mathbf{L} + 2\mathbf{S}|A\beta\rangle$, while the electric dipole terms are independent of spin with the selection rule $\Delta m_s = 0$.[30] Here, α and β represent spin-up and spin-down electrons, respectively. Addition of spin-orbit coupling enables rotation of light in the complex plane and gives rise to nonzero C terms. The specifics of this process will now be examined for the three different types of transitions.

First, the transition can be to a degenerate state of e symmetry which is group theoretically allowed in absorption. Spin-orbit coupling within the e manifold splits the degenerate pair by an amount λ where λ is the net spin orbit coupling constant of the delocalized final state. In the D_{2d} double group e splits into functions transforming as Γ_7 with $|m_J| = 3/2$ and Γ_6 with $|m_J| = 1/2$, while the b_2 ground state transforms as Γ_7 with $|m_J| = 1/2$. At low temperature only the $m_J = -1/2$ component of the ground-state Kramers doublet will be populated. The MCD selection rules are $\Delta m_s = 0$ and $\Delta m_J = \pm 1$ for positive or negative MCD sign, which implies that the $\Gamma_7(d_{x^2-y^2}) \rightarrow \Gamma_6(e)$ transition will exhibit a positive C term, while the $\Gamma_7(d_{x^2-y^2}) \rightarrow \Gamma_7(e)$ transition will have a negative C term. Since the $^2E \leftarrow {}^2B_2$ transition is fully group theoretically allowed with x,y polarization, the electric dipole terms m_x and m_y in eq 4 will be nonzero and equal to each other. Thus $|C|$ for both the Γ_7 and Γ_6 components will equal $(1/6)gm^2$ where the sum over the Zeeman operator in

(29) Pheipho, S. B.; Schatz, P. N. *Group Theory In Spectroscopy*; Wiley: New York, 1983.
(30) Gerstman, B. S.; Brill, A. S. *J. Chem. Phys.* **1985**, *82*, 1212.
(31) Solomon, E. I. *Comments Inorg. Chem.* **1984**, *3*, 225.
(32) Penner-Hahn, J.; Solomon, E. I.; Hodgson, K. O., to be published.
(33) While it is most appropriate to use the Gram–Schmidt technique for calculation of ground-state properties which are most sensitive to the ground-state function, MCD parameters can be affected by spin-orbit mixings into both ground and excited states. Thus, the Löwdin orthogonalization, which treats all orbitals equivalently, should also be considered.
(34) Hitchman, M. A.; Cassidy, P. J. *Inorg. Chem.* **1979**, *18*, 1745.
(35) Ferguson, J. *J. Chem. Phys.* **1964**, *40*, 3406.
(36) Rivoal, F.; Briat, B. *Mol. Phys.* **1974**, *27*, 1081.

eq 4 has been replaced by the g value. The electric dipole intensity D is given by

$$D = \frac{1}{6}\sum_{\alpha,\lambda}|\langle A\alpha|\mathbf{m}|J\lambda\rangle|^2 \quad (5)$$

which is equal to $(1/6)\cdot 2\cdot m^2$. Therefore $|C/D|$ is equal to $g/2$ for these transitions. Provided the spin-orbit splitting of the ^{2}E state is greater than the bandwidth, the MCD will then exhibit two transitions of equal magnitude but opposite sign, which is known as a pseudo A term.[37]

A second class of transitions in the D_{2d} $CuCl_4^{2-}$ complex concerns those that are group theoretically forbidden which includes transitions from $^2B_2$ to $^2B_1$, $^2B_2$ and $^2A_2$. Without spin-orbit coupling, the terms $\langle A\alpha|\mathbf{m}|J\lambda\rangle$ in eq 4 are zero, and no C-term intensity is expected. Out-of-state spin orbit coupling with the fully-allowed e states mixes some allowed x,y character in equal proportion into the forbidden states. In the D_{2d} double group, $^2B_1$ and $^2B_2$ transform as Γ_7 and will thus yield negative C terms while $^2A_2$ transforms as Γ_6 and gives rise to positive C terms. As C gains intensity in the same proportion as D, $|C/D|$ is again equal to $g/2$ for these transitions.

The final class for D_{2d} $CuCl_4^{2-}$ concerns nondegenerate transitions which are allowed in only one polarization. In D_{2d} $CuCl_4^{2-}$ this corresponds to the $^2A_1 \leftarrow {}^2B_2$ transitions which are allowed in z polarization. Equation 4 requires that $\langle A|m_i|J\lambda\rangle$ where $i = x,y,z$ be nonzero for at least two values of i to obtain C-term intensity and therefore, in the absence of spin-orbit coupling, C will be zero for these transitions. Turning on the spin orbit coupling will mix some allowed x or y character into states of a_1 symmetry. The $^2A_1$ state has Γ_6 symmetry in the D_{2d} double group, and the $^2A_1 \leftarrow {}^2B_2$ transition will thus have a positively signed MCD C-term. Unlike the previous two cases however $|C/D|$ will not equal $g/2$. The magnitude of C is proportional to the extent of spin-orbit coupling, while D is much larger since the transition is fully allowed. Thus $|C/D|$ will be small.

If spin-orbit coupling into the ground state is excluded, then the net MCD C term intensity will sum to zero over the excited states.[30] Inclusion of spin-orbit coupling with the ground state will give rise to a net C term intensity which, in the case of the states of e symmetry, will be proportional to the relative amounts of $d_{x^2-y^2}$ and d_{xy} character in the ground-state wave function. As very little d_{xy} is present in the spin-orbit mixed ground-state wave function, the imbalance between the positive and negative contributions to the C term is quite small.

There are several features of note arising from consideration of this last class of transitions. First, the magnitude of C/D will be strongly dependent on the magnitude of spin-orbit coupling. Thus, states mainly centered on atoms with higher spin-orbit coupling constants will in general give rise to larger C/D ratios than those centered on atoms with small spin-orbit constants. For example, we[38] have observed that ligand-field transitions in copper imidazole complexes exhibit C/D ratios approximately four to seven times larger than those from charge-transfer transitions where the ligand-field states are mainly copper centered (ξ_{Cu} = 828 cm^{-1}) and the CT transitions are mainly nitrogen centered (ξ_N = 75 cm^{-1}). A second feature is that C/D values will rise in magnitude as the transition moment decreases toward the limiting case of a forbidden transition. Finally, C/D values will also rise as states move closer together, increasing the spin orbit interaction between them.[30]

Turning to the Xα-MCD calculations for D_{2d} $CuCl_4^{2-}$, we need only consider the orbitally degenerate transitions as spin-orbit coupling within electric dipole-allowed ^{2}E states will dominate the MCD spectrum. Both the lowest and highest energy e CT transitions, 5e $\rightarrow$ $d_{x^2-y^2}$ and 3e $\rightarrow$ $d_{x^2-y^2}$, respectively, have most of the oscillator strength and are calculated with the lowest energy component of the pseudo A term having negative sign. The in-state spin orbit splitting of the 5e and 3e states is calculated to be 141 and 107 cm^{-1}, respectively. As this splitting is less than the experimental bandwidth ($\sim$2000 cm^{-1}), the observed $|C/D|$ will be less than $g/2$. The intermediate 4e $\rightarrow$ $d_{x^2-y^2}$ CT transition has a positively signed lowest energy component and a relatively small in-state splitting of 49 cm^{-1}.

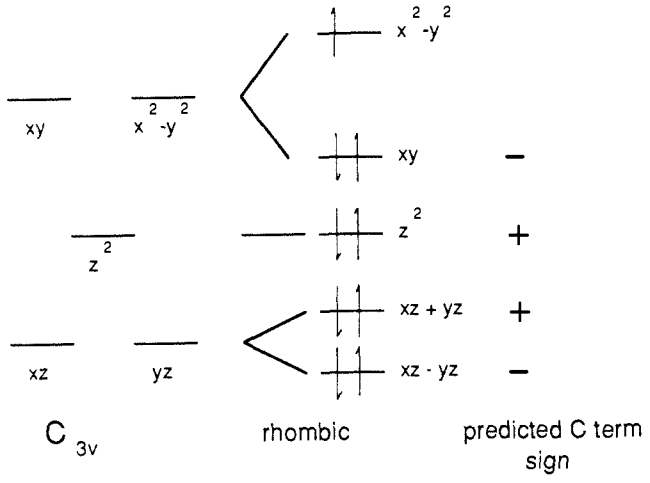

Figure 2. Ligand field d orbital splitting diagram of plastocyanin showing changes on going from C_{3v} symmetry to a rhombically distorted site. Predicted sign of the MCD C-term is given for each transition.

Experimentally,[36] the D_{2d} $CuCl_4^{2-}$ MCD spectrum is complicated by possible contributions from other copper species;[41] however, the lowest energy E state centered at 24 730 cm^{-1}, assigned as a (5e) Cl(π) $\rightarrow$ Cu($d_{x^2-y^2}$) transition, is split into negative and positive features with the negative feature to lower energy. Also in agreement with the calculation, the highest energy E state at 33 480 cm^{-1}, assigned as (3e) Cl(σ) $\rightarrow$ Cu($d_{x^2-y^2}$), has the negative feature to lowest energy. Thus, these MCD calculations of in-state spin orbit splitting strongly support our earlier[28] assignment of the bands at 33 480 and 28 880 cm^{-1} as deriving from σ and π Cl orbitals, respectively, rather than the previous proposal[36] that all the CT bands were due to π orbitals.

In summary, calibration of our approach using the assigned $CuCl_4^{2-}$ spectra indicates very good agreement between theory and experiment, especially for the charge-transfer region. We can now proceed to analysis of results for plastocyanin.

3.5. Application to the Blue Copper Site. A. Assignment of the Ligand-Field Region. The ligand-field transitions will dominate the low-energy spectral region of plastocyanin. Single-crystal spectral studies combined with ligand-field calculations[6] have indicated that the site has an approximately elongated C_{3v} geometry with some rhombic distortion. As shown in Figure 2 the transitions from the $d_{xz,yz}$ orbitals are predicted to be highest in energy and undergo a relatively small rhombic splitting. The d_{xy,x^2-y^2} levels are at lowest energy in C_{3v} with the rhombic perturbation causing a large splitting with the $d_{x^2-y^2}$ orbital going to higher energy. Finally, the d_{z^2} orbital transforms as a_1 in C_{3v} symmetry and thus is nondegenerate, but its energy is defined by the strength of the axial interaction (note that the thioether is oriented along the $C_3(z)$ axis).

With respect to qualitative predictions of the MCD C term intensity, we first note that all transitions in the blue copper site are group theoretically allowed and are to orbitally nondegenerate states. These transitions therefore have intrinsic moments in only one direction. Thus, the analysis of all blue copper transitions should follow the third case presented in the above section:

(37) Stephens, P. J. *Adv. Chem. Phys.* **1976**, *35*, 197.
(38) Gewirth, A. A.; Peterson, C. G.; Solomon, E. I., unpublished results.
(39) Kato, H. *Mol. Phys.* **1972**, *24*, 81.
(40) Greenwood, C.; Hill, B. C.; Barber, D.; Eglinton, D. G.; Thomson, A. J. *Biochem. J.* **1983**, *215*, 303.
(41) Both positive and negative features are expected in the C term contribution to the MCD from an e state. In the experimental spectrum for D_{2d} $CuCl_4^{2-}$, only a negative feature is observed corresponding to the lowest energy CT e state which peaks to lower energy than the corresponding absorption spectrum band. As no positive feature is observed, this indicates that the C term from this state is offset due to the presence of some paramagnetic contribution of opposite sign. MCD spectra of $CuCl_4^{2-}$ are thought to be sensitive to solvalyzed species, and tetragonal copper complexes are known to have strong negative MCD features in this region.[36,39,40]

spin-orbit coupling is required to mix in orthogonal transition moment character, giving rise to C term intensity with $|C/D| < g/2$. In particular, as noted above, states centered on atoms with large spin orbit coupling constants will generally yield larger C/D ratios than states centered on atoms with smaller spin orbit parameters. As $\xi_{3dCu} \sim 828\ cm^{-1} > \xi_{3pS} \sim 382\ cm^{-1} > \xi_{2pN} \sim 70\ cm^{-1}$, we again expect the largest C/D ratios from transitions located on dominately Cu-centered states (i.e., the d–d transitions). In D_{2d} symmetry, the lowest symmetry for which definitive group theoretical predictions of MCD signs can be made, the transition from the d_{z^2} level to the $d_{x^2-y^2}$ ground state is expected to have a positive C term, the d_{xy} level should give rise to a negative band, and the $d_{xz,yz}$ set will split giving rise to a pseudo A term. As the symmetry of the site is lowered from D_{2d}, the low symmetry can cause the d orbitals to mix, lift the degeneracy of the $d_{xz,yz}$ set, and complicate prediction of C term sign. However, as long as the low-symmetry splitting of the $d_{xz,yz}$ set is less than their average energy difference with the d_{xy} and d_{z^2} levels, the $d_{x^2-y^2} \rightarrow d_{z^2}$ transition will still have positive C term sign, while the transition to d_{xy} will still have negative sign. Further, Brill[30] has shown that even in lower symmetry the d_{xz+yz} and d_{xz-yz} orbitals[42] give rise to positive and negative C terms, respectively, as long as the d_{xz-yz} orbital is to lower energy than d_{xz+yz}. As the rhombically distorted C_{3v} plastocyanin site is expected[6] to exhibit a relatively small splitting in the $d_{xz,yz}$ set we can thus predict the transition from $d_{x^2-y^2}$ to d_{z^2} to have positive sign, $d_{x^2-y^2}$ to d_{xy} to have negative sign, and the close-to-degenerate $d_{xz,yz}$ set to exhibit a pseudo A term with the lower energy d_{xz-yz} orbital having negative sign. These predicted C term signs are given in Figure 2.

By using these predictions for the ligand-field transitions and assuming that no transitions occur at energies lower than the 5000-cm^{-1} cutoff in the spectrum,[43] we can now proceed with specific assignments. There are four transitions found in the low-energy part of the spectrum which can be assigned as ligand-field transitions based on their large MCD intensities, bands 5 through 8. The lowest energy negative MCD feature must be the $d_{xy} \rightarrow d_{x^2-y^2}$ transition which we can assign as band 7. The xz,yz transitions should appear at higher energy with a small low-symmetry splitting, similar C term intensity, and opposite signs and thus can be assigned as bands 5 and 6. Finally, this leaves the lowest energy transition, band 8, with a positive C term, as the $d_{z^2} \rightarrow d_{x^2-y^2}$ transition.

The Xα calculation in Tables II and III supports the experimental assignments presented above. The 17a′ ← 12a″ ($d_{xy} \rightarrow d_{x^2-y^2}$) transition is calculated to occur at 8691 cm^{-1} with a relatively large, negative C/D ratio, but relatively small oscillator strength consistent with experiment for band 7. (Note that the acceleration form calculation substantially overestimates the intensity of this transition.) Similarly, the 16a′ ← 12a″ ($d_{xz-yz} \rightarrow d_{x^2-y^2}$) transition calculated at 15 064 cm^{-1} also has a large negative C/D ratio and low oscillator strength as is observed for band 5.

Three valence levels in Table II have significant copper d_{z^2} character: 18a′, 15a′, and 13a′ with calculated transition energies of 4527, 15 895, and 36 700 cm^{-1}, respectively. The 18a′ and 13a′ levels are mostly methionine-centered levels and correspond to the HOMO b_2 and a_1 orbitals in the free ligand (vida infra). We find the mixing among these levels to be quite dependent on sphere size. In this adjusted sphere calculation the 18a′ level has significant d_{z^2} character (20%), and 15a′ is weakly bonding. Alternatively, with the Norman radii (ref 7, Table II) we calculate the 18a′ level to be essentially nonbonding and thus having no transition intensity to the ground-state $d_{x^2-y^2}$ orbital. Similarly, the Norman radii calculated, dominately copper-centered 15a′ level (labled 16a′ in Table II, ref 7) is found to be antibonding with the methionine a_1 level (14a′ in Table II, ref 7). While identification of band 8 with the transition from the 18a′ level is a possibility based on the calculated transition energy and a calculated positive C term for this transition, this assignment is excluded by the fact that stellacyanin, a blue copper protein which does not contain methionine, also exhibits this low-energy transition.[12] Thus, band 8 must be associated with the 15a′ ($d_{z^2} \rightarrow d_{x^2-y^2}$) transition which is also calculated to have a positive MCD C term but an energy significantly higher than is observed. This reduced transition energy observed in the MCD experiment is an indication of the d_{z^2} orbital being destabilized due to a more substantial interaction with the 13a′ orbital of the apical thioether then indicated in this adjusted sphere Xα calculation. Further, this calculation appears to overstate the amount of d_{z^2} character in the 18a′ ligand orbital.

Finally, the 11a″ level (d_{xy+yz}) has a small, positive C/D ratio, a transition energy of 11 942 cm^{-1}, and the second largest calculated oscillator strength, in agreement with the experimental assignment of band 6. In earlier spectral studies of blue copper centers, this band had been assigned as the lowest energy cysteine charge transfer transition due to its relatively high intensity. The source of intensity in this "d–d" transition is considered in the next section.

B. Assignment of Thiolate Charge-Transfer Transitions. We now consider the specific valence orbitals involved in the thiolate charge-transfer process and their contribution to the absorption spectrum in Figure 1. Previously[6] we associated the three nondegenerate orbitals predicted for the thiolate–copper bond (π, pseudo-σ, and σ, in order of increasing energy) with the three most intense bands in the blue copper spectrum in Figure 1A (bands 6, 4, and 3, respectively); the pseudo-σ orbital being associated with band 4 with the highest intensity as it is most oriented along the S–Cu bond and the π orbital associated with the moderately intense band 6. However, assignment of band 6 as the $d_{xz+yz} \rightarrow d_{x^2-y^2}$ transition (vida supra) requires that this assignment be revised. In the adjusted sphere Xα calculated presented here, transitions from the cysteine π (10a″), pseudo-σ (14a′), and σ (12a′) orbitals to the $d_{x^2-y^2}$ orbital are calculated to be at 16 940, 25 313, and 47 685 cm^{-1}, respectively. A most interesting feature to come from these calculations is that the lowest energy S pπ CT is predicted to be the most intense band in the absorption spectrum. As bands 5–8 are experimentally assigned as d–d transitions, and band 4 is the most intense band in the absorption spectrum, it is logically assigned as the lowest energy S p$\pi \rightarrow d_{x^2-y^2}$ CT transition. The calculated C/D ratio in Table III for this transition is one of the lowest also in agreement with experiment. Note that while the calculated sign is positive and the observed MCD sign of band 4 is negative, the very low calculated C term intensity is strongly influenced by small differences in spin-orbit mixing with other states which may not be quantitatively modeled in this calculation.

The large absorption intensity in this transition derives from the extremely good overlap between the ground-state $d_{x^2-y^2}$ orbital which is antibonding with the Sπ orbital of the thiolate (12a″: 36% Sπ character) and the bonding thiolate π excited-state level (10a″: 21% Sπ character). The contour diagrams of these orbitals are given in Figure 3. Finally, we note that the transition moment associated with the intense S pπ CT transition is directed along the Cu–S(cys) bond in both oscillator strength calculations in agreement with our polarized single crystal absorption data on band 4 in ref 6.

As indicated above, while the relatively high intensity of band 6 originally led to its assignment as the lowest energy cysteine π CT transition, it has now been experimentally assigned as a d–d transition involving the 11a″ level. These adjusted sphere Xα calculations provide an explanation for the high intensity of this ligand-field transition. Band 6 is associated experimentally with the $d_{xz+yz} \rightarrow d_{x^2-y^2}$ ligand-field transition on the basis of the sign of the MCD transition. However, this d_{xz+yz} orbital has the correct symmetry (a″) and phase to allow for configuration interaction and thus mixing with the thiolate sulfur pπ 10a″ orbital. The Xα calculated S pπ character in the 11a″ (d_{xz+yz}) orbital is 14%, and this accounts for the relatively high oscillator strength associated with the transition from this orbital (I_6/I_4: obsd = 0.23, calcd = 0.58).

(42) Note that we rotate the coordinate frame 45° relative to that used in Brill's paper[30] so that the ground state is now $d_{x^2-y^2}$.

(43) The existence of electronic transitions to lower energy than 5000 cm^{-1} would require g values substantially larger than those observed experimentally.

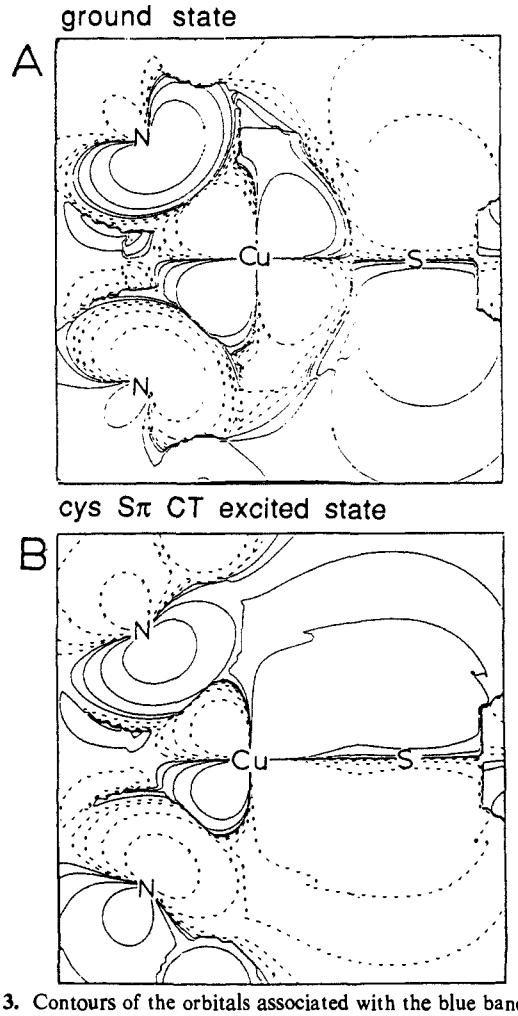

Figure 3. Contours of the orbitals associated with the blue band transition in plastocyanin: (A) ground-state 12a″ orbital and (B) excited-state 10a″ orbital. Values of the contours are ±0.003, ±0.009, ±0.027, and ±0.081.

The remaining two thiolate orbitals could contribute to higher energy in the absorption spectrum. The highest energy of these, from the σ orbital (12a′), is stabilized by 30 745 cm^{-1} in the C_s(met) calculation and 36 135 cm^{-1} in the methanethiol free ligand relative to the cysteine S pπ level. It is thus not expected to contribute in the accessible spectral region (i.e., below the 280-nm intense protein absorption). To lower energy is the "pseudo-σ" orbital (14a′) with a calculated transition energy of 25 313 cm^{-1}, only 8373 cm^{-1} above the π level. In contrast to earlier predictions that this should be the most intense CT transition, the 14a′ level has little overlap with the ground-state 12a″($d_{x^2-y^2}$) level as 12a″ only contains S pπ character. Thus the 14a′ level in fact has little oscillator strength but could gain limited intensity through low-symmetry mixing with the 10a″ π band (the actual Cu site symmetry in plastocyanin is C_1). This would produce absorption intensity polarized along the Cu–S(cys) bond. Two bands in the absorption spectrum (2 and 3) lie to higher energy from the blue band and are candidates for the cysteine CT transition associated with the pseudo-σ orbital. While the $I_\parallel/I_\perp$ ratio with respect to the crystallographic *a* axis for band 2 is too high to be associated with transitions polarized along the Cu–S(cys) bond,[6] band 3 does exhibit the correct polarization behavior. Further, the splitting between bands 4 and 2 varies substantially among azurin, stellacyanin, and plastocyanin; however, the splitting between bands 3 and 4 is relatively constant.[12] Band 3 is therefore assigned as the cysteine pseudo-$\sigma \rightarrow d_{x^2-y^2}$ (14a′ → 12a″) CT transition.

Three weak bands (0–2) remain to be considered in the blue copper spectrum, and these must correspond to CT transitions from low-lying valence orbitals of the remaining two imidazole and thioether ligands.

As explained previously,[7,44] three valence levels from an imidazole are involved in bonding to the copper: a carbon-centered π_1, a nitrogen-centered π_2, and a σ orbital on the coordinated nitrogen. In order to probe the imidazole transitions we have performed calculations replacing one of the amines in the C_s(met) site with imidazole in the same orientation as in the C_s(his) calculation described in ref 7. Xα calculation of these levels is difficult, as the large imidazole ligand places much charge density in the intersphere region. In addition, the splitting and energies of the π_1 and π_2 levels are subject to wide variation depending on choice of the sphere radius of the copper-coordinated imidazole nitrogen (in contrast to the behavior exhibited by the thiolate levels). Model studies of Schugar[45] indicate that imidazole can contribute in the region between 20 000 and 40 000 cm^{-1}. Adjusting the radius of the copper-coordinated nitrogen center to 2.0 bohr places transitions from π_1 and π_2 at 14 770 and 52 894 cm^{-1}, respectively. This does suggest that the histidines should contribute in the visible region. It should be noted that both π orbitals are perpendicular to the $d_{x^2-y^2}$ orbital and have limited overlap. Thus neither transition mixes into the ground state and hence its description in the C_s(met) calculation is not affected by approximating amine for histidine, and both π CT transitions should have very little intensity, the π_1 being lowest. Of the remaining weak bands, band 2 is polarized consistent with contributions from the histidines[6] and has a reasonable energy[45] for a π_1 to Cu $d_{x^2-y^2}$ transition. Finally, the model studies and the calculation also indicate that the higher energy band zero could be associated with a CT transition from the π_2 level of histidine.

The remaining ligand is the thioether which contributes three valence orbitals. At lowest energy is the b_2 level which corresponds to an S pπ orbital which is perpendicular to the C–S–C plane and is nonbonding. Next in energy is the S pσ (a_1) which extends out of the S end of the thioether molecule in the molecular plane. The separation between these two levels in the PES spectrum[46] of the free ligand is 20 568 cm^{-1}. At highest energy is the b_1 level which is strongly involved in bonding to the methyl groups and thus is 1.4 eV below the a_1 level. Upon coordination to the metal in the blue copper site, the b_2 corresponds to the 18a′ level with a transition energy of 4527 cm^{-1}, the a_1 corresponds to the 13a′ at 36 700 cm^{-1}, and the b_1 is next at 55 223 cm^{-1} which is not in the accessible spectral region. As discussed earlier, the 18a′ level is predicted to be the lowest energy transition while the 13a′ is predicted to be 11 000 cm^{-1} above the cysteine pseudo-σ level. Both transitions have little overlap with the $d_{x^2-y^2}$ ground states and thus are expected to have limited intensity. In Table III, the 13a′ level is calculated to have an order of magnitude more intensity than the 18a′ level—comparable to that of the cysteine S pseudo-σ and some of the d–d transitions which are observed with $\epsilon \sim 400$ M^{-1} cm^{-1}. Model studies[47] assign a band between 22 700 and 27 500 cm^{-1} as arising from a transition between this level and the ground state. Band 1 at 23 440 cm^{-1} exhibits polarization behavior[6] consistent with a transition polarized along the Cu–S(met) bond and is in the correct energy range to be associated with a charge transfer from the methionine a_1 orbital.

The assignments of all the bands in the blue copper spectrum are included in Figure 1A.

3.6. Relation to Other Blue Sites. The thiolate copper bond can change in other proteins containing blue sites leading to variations in thermodynamic and kinetic properties and changes in spectroscopic features relative to plastocyanin. Two other blue proteins, stellacyanin and azurin, have well-characterized[12] ab-

(44) Fawcett, T. G.; Bernarducci, E. E.; Krogh-Jesperson, K.; Schugar, H. J. *J. Am. Chem. Soc.* **1980**, *102*, 2598.

(45) (a) Schugar, H. J. In *Copper Coordination Chemistry: Biochemical and Inorganic Perspectives*; Karlin, K. D., Zubieta, J., Eds.; Adenine: Guilderland, NY, 1983; p 43. (b) Knapp, S.; Keenan, T. P.; Zhang, X.; Fikar, R.; Potenza, J. A.; Schugar, H. J. *J. Am. Chem. Soc.* **1987**, *109*, 1882.

(46) Frost, D. C.; Herring, F. G.; Katrib, A.; McDowell, C. A.; McLean, R. A. N. *J. Phys. Chem.* **1972**, *72*, 1036.

(47) Nikles, D. E.; Anderson, A. B.; Urbach, F. L. In *Copper Coordination Chemistry: Biochemical and Inorganic Perspectives*; Karlin, K. D., Zubieta, J., Eds.; Adenine Press: Guilderland, NY, 1983; pp 167–202, and references therein.

Table V. Results of Xα-SW Calculation of Change in Blue Band ($10a'' \rightarrow 12a''$) and $d_{xy} \rightarrow d_{x^2-y^2}$ ($17a' \rightarrow 12a''$) Transition Energies (cm^{-1}) for Three Distortions in Cu-S(cys) Bonding Relative to C_s(met) Calculation[a]

distortion	Δblue band	$\Delta d_{xy} \rightarrow d_{x^2-y^2}$
Cu-S(cys) = 2.20 Å	-1048	-220
Cu-S(cys) = 2.06 Å	+2547	+757
Cu-S(cys)-C = 104°	+20	-92
Cu-S(cys)-C = 114°	+5	+13
S(met)-Cu-S(cys)-C = 10°	-319	-372

[a] Original values in C_s(met) calculation: Cu-S(cys) = 2.13 Å; Cu-S(cys)-C = 109°; S(met)-Cu-S(cys)-C = 0°.

sorption spectra, and it is important to consider the structural differences which account for the spectral differences between these proteins and plastocyanin. The above assignment indicates that most of the absorption intensity arises from the cys $S\pi \rightarrow d_{x^2-y^2}$ charge-transfer transition (10a'), and it is thus necessary to correlate changes in this spectral feature with different possible distortions of the cys S-Cu bond. In addition, the ligand field bands are also observed to shift in energy between different blue copper proteins. Three distortions relating to the thiolate ligand are possible: (1) the Cu-S bond length can change, (2) the cu-S-C bond angle can change, (3) the S(met)-Cu-S(cys)-C(cys) dihedral angle can vary from its near 0° value in the plastocyanin crystal structure.

In order to probe the effect of these distortions on the spectra, we have performed additional Xα-SW calculations on the C_s(met) geometry altered as indicated above, and Table V presents the corresponding changes in transition energy for both the blue band and a representative ligand-field ($d_{xy} \rightarrow d_{x^2-y^2}$) transition. For the distortions involving a change in angle the sphere radii were left constant, while, for the stretches, sphere radii were scaled so as to retain constant overlap between the Cu and S(cys) spheres.[48] Table V indicates that neither the ligand field nor the blue band is particularly sensitive to changes in the Cu-S-C bond angle. Alternatively, the blue band is strongly affected by changes in the S-Cu bond length, while the change in energy of the ligand field band for this distortion is more limited. Finally, both the ligand field and blue band transitions shift by a comparable amount for the S(met)-Cu-S(cys)-C torsion.

4. Discussion

The above assignment of the plastocyanin absorption spectrum indicates that the dominant CT intensity is due to a transition from the cysteine π bonding orbital to the half-occupied ground-state $d_{x^2-y^2}$ orbital containing substantial cysteine π antibonding character. The intensity in this transition arises from the good overlap of the excited state cysteine sulfur π bonding orbital with the ground state cysteine sulfur π antibonding orbital. The other transitions in this region gain intensity through mixing with this π transition. In particular, band 6 is the $d_{xz+yz} \rightarrow d_{x^2-y^2}$ transition which has significant S pπ mixing.

Alternatively, the dominant MCD intensity in plastocyanin as measured through C/D ratios is associated with the ligand-field transitions. Since all the plastocyanin transitions are allowed, and nondegenerate, MCD C terms come about through spin orbit coupling. The greater C/D ratios for ligand field bands thus requires more spin orbit induced orthogonal transition moment character in this spectral region than in the charge-transfer region. The highest spin-orbit coupling is expected on metal-centered states, since copper has the largest spin orbit coupling constant of the atomic centers in the plastocyanin active site. As mentioned above, similar behavior has been observed for copper-imidazole complexes.

There are several important features in the assignment presented here which give insight into the bonding in the plastocyanin active site. With respect to the ligand field region, a previous crystal field calculation[6] indicated that the plastocyanin site should be viewed as having elongated C_{3v} effective symmetry with rhombic

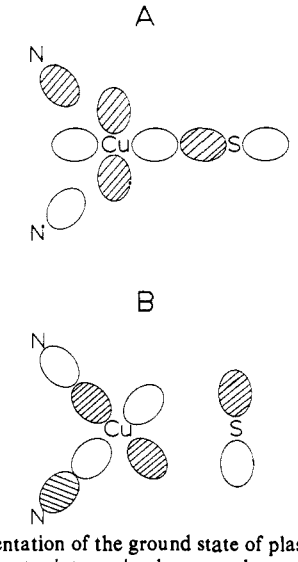

Figure 4. Representation of the ground state of plastocyanin: (A) early model with dominant σ interaction between the copper and the cysteine p_z sulfur orbital and (B) present model with strong π interaction between the copper $d_{x^2-y^2}$ and cysteine pπ sulfur orbitals. Note rotation of $d_{x^2-y^2}$ ground state by 45°.

distortions. The experimental assignment of the d_{xy} orbital below the $d_{xz,yz}$ set provides additional confirmation of this picture and provides information on the nature of the rhombic distortions present in the site. In particular, the substantial destabilization of the $d_{x^2-y^2}$ orbital relative to the d_{xy} level emphasizes the strength of the cysteine sulfur π antibonding interaction in the ground state which, in fact, causes this rhombic splitting. In ref 7, the antibonding interaction between the cysteine sulfur π level and $d_{x^2-y^2}$ was found to be responsible for the ground-state properties of the plastocyanin site.

Second, the assignment of the d_{z^2} orbital as the lowest excited d orbital, band 8, indicates that there is a reasonable interaction between the thioether and the copper. This destabilization is consistent with the decrease in energy of the d_{z^2} transition going from D_{4h} $CuCl_4^{2-}$ to D_{4h} $CuCl_6^{4-}$ where apical chlorides at 2.95 Å are added (discussed in ref 7). It is important to consider the role of this axial ligation in other blue proteins. In azurin, the Cu-S(met) bond length is ~3.1 Å[49] compared with 2.9 Å in plastocyanin. One would thus expect the axial destabilization of the d_{z^2} orbital to decrease in azurin relative to that in plastocyanin. Experimentally,[12] all ligand field bands in azurin except band 8 are ~500 cm^{-1} lower in energy relative to those in plastocyanin. This lowest energy band however increases in energy going from plastocyanin to azurin by ~500 cm^{-1} supporting its assignment as the $d_{z^2} \rightarrow d_{x^2-y^2}$ transition.

With respect to the blue band, band 4, its assignment as arising from a cysteine $\pi \rightarrow$ Cu $d_{x^2-y^2}$ transition represents an important evolution in developing an understanding of the blue copper active site. Originally, it was thought that the most destabilizing interactions between the thiolate sulfur and the copper would be between the σ orbital on the sulfur and $d_{x^2-y^2}$ as shown in Figure 4A. This would orient the $d_{x^2-y^2}$ orbital with a lobe along the Cu-S(cys) bond and would lead to an assignment of the blue band (band 6) as coming from a σ orbital as this level would now have the best overlap with the ground state, and CT intensity derives from the overlap of the donor and acceptor orbitals involved in the CT process. A lower energy, doubly degenerate π level was then associated with band 4. However, polarized optical studies[6] indicated that most of the intensity between bands 3 and 6 was polarized along the Cu-S(cys) bond, and since this region contains more than two transitions, the bonding of the thiolate had to be considered in more detail. In particular, the Cu-S-C bond angle found in the plastocyanin crystal structure is 109° which would cause one of the thiolate S pπ orbitals (that in the Cu-S-C plane)

(48) Cook, M. R. Ph.D. Thesis, Harvard University, 1981.

(49) Norris, G. E.; Anderson, G. F.; Baker, E. N. G. *J. Am. Chem. Soc.* **1986**, *108*, 2784.

to become pseudo-σ bonding to the copper (see Figure 5 in ref 7). Thus, three nondegenerate orbitals are predicted for the thiolate–copper bond (π, pseudo-σ, and σ, in order of increasing energy), and, indeed, the photoelectron spectrum of methanethiol which has a 107° H–S–C bond angle does show three transitions from the sulfur.[46] In ref 7 we considered these valence orbitals of the thiolate to be associated with the three most intense bands in the blue copper spectrum in Figure 1A (bands 6, 4, and 3, respectively) with the pseudo-σ being associated with the band with the highest intensity as it is most oriented along the S–Cu bond. Finally, as indicated above, we find the cysteine S pπ orbital to play the dominant role (i.e., antibonding interaction) in orientating the $d_{x^2-y^2}$ orbital resulting in lobes at 45° relative to the Cu–S bond. This rotation of the thiolate orbital (Figure 4B) is required by both crystal field[6] and Xα calculations and is supported by the observation of at least one nitrogen superhyperfine coupling in the blue proteins at least as strong as those in tetraimidazole complexes (where the $d_{x^2-y^2}$ orbital points directly at the imidazole).[50] This changes the intensity mechanism, which derives from this overlap, so that now the Sπ to $d_{x^2-y^2}$ transition is most intense.

The assignment of the blue band as pictured in Figure 1 also provides insight into changes in geometry upon optical excitation which in turn contribute intensity to the resonance Raman spectrum associated with this transition. In particular, one is taking an electron out of a π bonding orbital and putting it into a π^* orbital with respect to the copper. Clearly, elongation of the Cu–S(cys) bond and thus vibrational enhancement of the Cu–cys stretch is predicted which however may be strongly mixed with other modes.[9,51,52] Further, loss of this π bond leads to the possibility of a dihedral distortion around the S(met)–Cu–S(cys)–C(cys) torsion upon excitation. It is not clear at this point where this mode would contribute to the vibrational spectrum. Alternatively, no distortion in the Cu–S–C angle is expected. In quantitative agreement with the above considerations, the changes in transition energy given in Table V for each of these distortions can be considered to be a reasonable estimate of the distorting force $\langle\psi_{S\pi}|(\partial V/\partial Q_i)_0|\psi_{S\pi}\rangle$ where Q_i is each mode of vibration. The excited distortion is thus given as $\Delta Q_i = \langle\psi_{S\pi}|(\partial V/\partial Q_i)_0|\psi_{S\pi}\rangle/k_i$ where k_i is the force constant of Q_i. From Table V, this quantity is largest for the Cu–S stretch, still of reasonable magnitude for the dihedral torsion, and essentially zero for the Cu–S–C bend.

In summary, the thiolate copper bond plays a dominant role in defining the electronic structure of the blue copper active site with respect to orientation and delocalization of the ground state and the electronic excited states. Changes in this bond clearly change spectral features and could contribute to variation in reactivity of blue copper sites both with respect to electron-transfer pathways and variation in redox potentials of blue sites in different proteins.

Acknowledgment. We thank Dr. Michael R. Cook for helpful discussions on the Xα calculations. Funding of this work by the NSF (CHE-86-13376) is gratefully acknowledged. Calculations were (in part) supported by Grant no. CHE-83-12693 from the National Science Foundation.

Registry No. Cu, 7440-50-8.

(50) (a) Roberts, J. E.; Cline, J. F.; Lum, V.; Freeman, H. C.; Gray, H. B.; Peisach, J.; Reinhammer, B.; Hoffman, B. *J. Am. Chem. Soc.* **1984**, *106*, 5324. (b) The most recent crystallographic coordinates of plastocyanin[53] give a short 1.95 Å Cu–N bond length for the coordinated nitrogen of His37 and a S(cys)–Cu–N(his37) bond angle of 132° which coupled with the orientation of the ground-state $d_{x^2-y^2}$ orbital[7] implies that this nitrogen lies directly along one of the $d_{x^2-y^2}$ lobes. However, the coordinated nitrogen of His87 has a relatively long 2.09 Å bond length with a S(cys)–Cu–N(his87) bond angle of 123° which implies that this nitrogen lies off one of the $d_{x^2-y^2}$ lobes. This is consistent with the reduced superhyperfine for one of the nitrogens observed experimentally in (a).

(51) Thamann, T. J.; Frank, P.; Willis, L. J.; Loehr, T. M. *Proc. Natl. Acad. Sci. U.S.A.* **1982**, *79*, 6396.

(52) Nestor, L.; Larrabee, J. A.; Woolery, G.; Reinhammer, B.; Spiro, T. G. *Biochem.* **1984**, *23*, 1084.

(53) Freeman, H. C., to be published.